

Characterization of deep-levels in silicon nanowires by low-frequency noise spectroscopy

Abhishek Motayed,^{a)} Sergiy Krylyuk, and Albert V. Davydov

National Institute of Standards and Technology, Material Measurement Laboratory, Gaithersburg, Maryland 20899, USA

(Received 24 May 2011; accepted 10 August 2011; published online 13 September 2011)

We have used low-frequency noise (LFN) spectroscopy to characterize generation-recombination (G-R) centers in silicon nanowires grown using chemical vapor deposition. The LFN spectra showed Lorentzian behavior with well-defined corner-frequency indicative of single G-R center in the bandgap. From the temperature-dependent LFN measurement a single deep level at 0.39 eV from the bandedge is identified, which matches closely with the Au donor level in Si. The trap concentration was estimated at $2.0 \times 10^{12} \text{ cm}^{-3}$ with electron and hole capture cross-sections of $9.5 \times 10^{-17} \text{ cm}^2$ and $1.4 \times 10^{-16} \text{ cm}^2$, respectively. This study demonstrates the potential of the LFN spectroscopy in characterization of deep-levels in nanowires. © 2011 American Institute of Physics. [doi:10.1063/1.3637049]

In the last decade semiconductor nanowire (NW)-based devices have evolved from simple back-gated field-effect transistors (FETs) to the state-of-the-art vertically integrated FET, resulting in significant improvement in their performance.^{1,2} However, the measurement techniques for electrical properties (mobility, carrier concentration, electrically active defects) are lagging when compared to the innovations made in the material properties characterization for the nanowire field in general. Electrical properties of NWs such as carrier type, mobility, and concentration are often estimated from the parametric measurements of FET devices.³ Unfortunately, such measurements do not reveal any information regarding the carrier generation-recombination (G-R) mechanisms via deep-levels. Besides band-to-band excitation and recombination, carrier recombination via deep-levels in the bandgap often determines the device performance.⁴ Traditionally, deep-level transient spectroscopy (DLTS) is used to measure the G-R centers or deep-levels in bulk/thin-film semiconductors.⁵ Forming Schottky diodes with capacitance values greater than 10^{-14} F is often difficult in nanowire devices due to the size of the nanowire, making DLTS measurement impractical. By measuring noise power spectral density (PSD) of the dc current flowing through a semiconductor, one can estimate energy level, time-constants, and density of the G-R centers present in the sample.⁶ Low-frequency noise or “spontaneous fluctuations” in current through semiconductors exists due to the stochastic nature of the conduction process and was first studied in details by Van Der Ziel.⁷ Later, the theory of fluctuations due to G-R centers in Si junction FETs was successfully developed by Lauritzen and Shah.⁸ Copeland finally developed the equations necessary for extraction of the trap parameters in *n*-type GaAs.⁹ This theory was further refined and employed by Scholz *et al.* for characterization of deep and shallow levels in Si.⁶ Although recently low-frequency noise (LFN) has been measured for Si, ZnO, GaN, InAs, and SiGe NW FETs,^{10–14} this powerful technique has not been used to

determine the deep-level characteristics. Only limited temperature-dependent LFN measurements have been reported by few authors.^{11,13,15}

In this letter, we demonstrate the potential of temperature-dependent LFN spectroscopy to probe deep levels in NWs. We detected a single deep level in the bulk of silicon nanowires (SiNWs) located at 0.39 eV from the bandedge, which is in a good agreement with the energy of the Au donor level in Si, and estimated its electron and hole capture cross-sections as well as the trap concentration.

The SiNWs used in this study were grown at 850 °C from $\text{SiCl}_4/\text{H}_2/\text{N}_2$ gaseous mixture using Au nanoparticles as catalyst.¹⁶ The p-type SiNWs were obtained by boron doping using B_2O_3 powder. Post-growth device fabrication was done by dielectrophoretically assembling the nanowires on a heavily doped p-type Si substrate which had 1.2 μm thick thermally grown SiO_2 on top of it.¹⁶ After the alignment, 50 nm of SiO_2 was deposited using plasma-enhanced chemical vapor deposition, and back-gated FET devices were fabricated using standard microfabrication processes.¹⁶ The LFN measurement was done in an open-cycle cryogenic probestation. The drain and gate bias was provided by the Agilent B1500A semiconductor parameter analyzer, and the channel current was converted to voltage using SRS 570 low-noise current amplifier.¹⁷ The voltage output from the amplifier was connected to a HP 3561A dynamic signal analyzer. After the electrical measurements were complete, the top SiO_2 layer was removed by reactive ion etching. The nanowire dimensions were measured in a field-emission scanning electron microscope (FESEM) in order to estimate the mobility and the carrier concentration in the nanowires.

Figures 1(a) and 1(b) show the I_{DS} vs. V_{DS} characteristics of a SiNW FET (diameter 192 nm) at 310 K and 200 K, respectively. Besides the obvious fact that the current at 200 K has decreased from 300 K approximately by a factor of 10, no other information about the carrier dynamics can be obtained. The field-effect hole mobility (μ) calculated for all the nanowires were in the range of $(0.5\text{--}4.0) \text{ cm}^2 \text{ V}^{-1} \text{ s}^{-1}$. The low hole mobility values in these nanowires is surprising considering the hole concentration calculated for these

^{a)}Author to whom correspondence should be addressed. Electronic mail: amotayed@nist.gov.

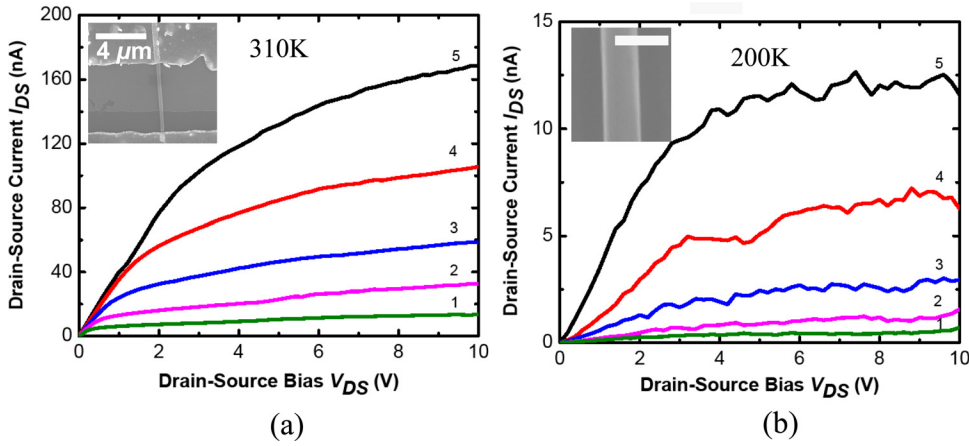


FIG. 1. (Color online) I_{DS} vs. V_{DS} characteristics as a function of gate voltage V_{GS} for a SiNW FET with diameter 192 nm and length 6 μm (a) at 310 K, and (b) at 200 K. Plots 1, 2, 3, 4, and 5 are for $V_{GS} = +10, +5, 0, -5, \text{ and } -10$ V, respectively. Insets in (a) and (b) show, respectively, low- and high-magnification FESEM images of the SiNW device. The scale bar in the inset in (b) is 300 nm.

SiNWs were fairly low, in the range of $(2.0\text{--}3.0) \times 10^{17} \text{ cm}^{-3}$. Possible scattering on extended structural defects was ruled out given that these nanowires are single-crystalline with very low defect density.¹⁶ Also, surface scattering can not be the dominant factor for such large diameter nanowires.¹⁸ There are few reports of low hole mobility values in boron-doped SiNWs which are in the same range as ours.^{19,20} From the Arrhenius plot of the two-terminal resistance of the same NW (see supplementary material²⁷) a good fit to the activation energy model is found, indicating a semi-conducting behavior. The point to be made here is that even the temperature-dependent I-V measurements do not reveal any information regarding the trapping mechanism. The normalized drain-current noise PSD S_I/I_{DS}^2 (i.e., $S_I = \langle i_{ds}^2 \rangle / \Delta f I_{DS}^2$, where $\langle i_{ds}^2 \rangle$ is the mean-square value of the fluctuations, Δf is the bandwidth, and I_{DS} is the dc drain current) for the same SiNW FET for four different temperatures is shown in Fig. 2. Typically for device exhibiting $1/f$ -type noise, the normalized noise PSD can be described by the relationship $S_I/I_{DS}^2 = \alpha_H/Nf^\beta$, where α_H is the Hooge constant, N is the total number of carriers, and exponential factor β is ideally 1.¹¹ At room-temperature the drain current noise PSD in these SiNWs clearly showed a Lorentzian-behavior, i.e., $S_I = A/(1 + f/f_0)$, where A is the low-frequency amplitude and f_0 is the characteristics frequency. The evolution of the spectrum from the Lorentzian to $1/f$ can be clearly seen at 200 K in Fig. 2. This behavior is representative of 20 single nano-

wire FETs fabricated from the same growth run. The thermal noise ($S_{thermal} = 4k_B T/R$) in these NW FETs is $\approx 10^8$ times smaller than the G-R noise and hence is neglected in the analyses. The estimated Hooge constant is 0.2 at 200 K with $\beta = 1.4 \pm 0.01$. The G-R noise seen in the PSD is independent of the gate bias as seen in the inset of Fig. 3, which identifies the noise to be originating in the bulk of the SiNW.²¹ In silicon, the common shallow dopants (boron, phosphorus) are completely ionized at room-temperature; thus, there are no fluctuations in the occupancy of these levels except at very low temperatures (< 10 K). However, in the presence of deep-level defects, fluctuations in the total number of carriers due to G-R process is prominent at moderate-temperatures with a time-constant τ ($\tau = 1/2\pi f_0$), which can be related to the trap energy-level and capture cross-section by the relationships⁶:

$$\ln(T^2\tau) \approx \left(\frac{\Delta E}{k_B T}\right) - \ln\left[\left(\frac{4k_B^2\sigma_n}{gh^3}\right)(6\pi^3 m_e^{1/2} m_h^{3/2})^{1/2}\right], \quad (1)$$

$$\ln(T^2\tau) \approx \left(\frac{\Delta E}{k_B T}\right) - \ln\left[\left(\frac{4k_B^2\sigma_p}{gh^3}\right)(6\pi^3 m_e^{3/2} m_h^{1/2})^{1/2}\right], \quad (2)$$

where ΔE is the trap-energy, σ_n and σ_p are the electron and hole capture cross-sections, respectively, g is the degeneracy

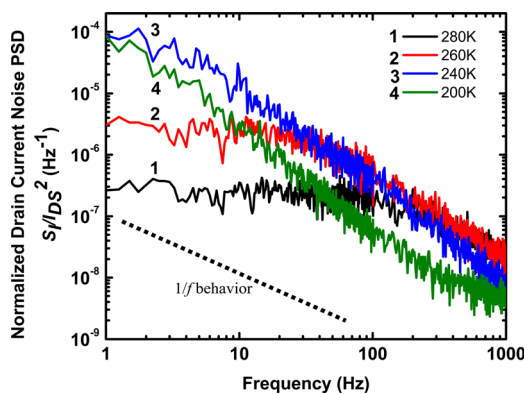


FIG. 2. (Color online) Normalized PSD of the drain current noise of the SiNW FET shown in Fig. 1 at four different temperatures. At room-temperature clear G-R behavior with Lorentzian distribution can be seen. At 200 K the noise changes to $1/f$ type with Hooge constant 0.2. The dashed line represents $1/f$ behavior.

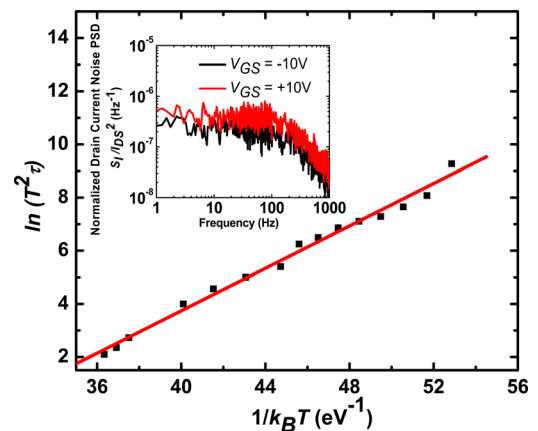


FIG. 3. (Color online) The Arrhenius plot of the $\ln(T^2\tau)$ vs. $1/k_B T$ showing good fit to the Eq. (1). The τ at every temperature is determined by fitting the LFN plot measured at that temperature to a Lorentzian distribution. (inset) Normalized PSD of the drain current noise of the SiNW FET shown in Fig. 1 at $V_{GS} = +10$ V and -10 V exhibiting no gate-bias dependence, which indicates bulk origin of the G-R noise.

factor, and m_e and m_h are the electron and hole masses, respectively. From the slope of the plot of $\ln(T^2\tau)$ vs. $1/k_B T$ (Fig. 3) we can extract the energy position of the trap-level, and the intercept will give us the capture cross-sections. From the plot in Fig. 3 we see a good fit to Eq. (1) with computed trap energy to be $0.39 (\pm 0.01)$ eV. It is well-established that Au has two deep-levels in silicon, a donor level at 0.35 eV from the valence band, and an acceptor level at 0.54 eV from the conduction band. In p-type Si only the donor level at 0.35 eV is active.²² The electron and hole capture cross-sections computed from the curve using Eqs. (1) and (2) are 9.5×10^{-17} cm² and 1.4×10^{-16} cm², respectively, assuming g to be 1. The reported values of electron and hole capture cross-sections for Au in Si are in the range of 10^{-16} to 10^{-15} cm².⁴ The values of degeneracy factors of deep-levels such as Au in Si are much debated.²³ While the uncertainty in the degeneracy factors does not affect the determination of the trap energy, it would affect the capture cross-sections and trap density. Once the capture cross-section is determined, the trap-concentration N_T can be determined for a p -type material (assuming $N_A \gg N_D$) using the following simplified relationship $\tau \approx 1/(\sigma_e v_e N_T)$, where v_e is the thermal velocity of the electrons given by $v_e = \sqrt{3k_B T/m_e}$.²² The trap concentration calculated from the capture cross-sections using the above relationship is 2.0×10^{12} cm⁻³. This value is 3 orders of magnitude lower than the equilibrium solubility of gold in silicon at 850 °C ($\approx 2 \times 10^{15}$ cm⁻³) as calculated from the thermal diffusion data.²⁴ It has been recently shown that during the vapor-liquid-solid (VLS) growth Au-catalyst could incorporate into SiNWs at concentrations equal to or even higher than the equilibrium solubility level.^{20,25} The observed discrepancy could be either due to the actual lower Au concentration in the SiNW matrix or due to the hydrogen passivation of Au traps.²⁶ This study identifies the LFN spectroscopy as an alternative to DLTS and optical measurements for characterization deep-levels in SiNWs and in other semiconductor nanowire materials.

This work was partially supported by the DTRA, Basic Research Award No. HDTRA1-10-1-0107, to the University of Maryland.

- ¹S.-W. Chung, J.-Y. Yu, and R. J. R. Heath, *Appl. Phys. Lett.* **76**, 2068 (2000).
- ²J. Goldberger, A. I. Hochbaum, R. Fan, and P. Yang, *Nano Lett.* **6**, (2006).
- ³A. Motayed, M. He, A. V. Davydov, J. Melngailis, and N. Mohammad, *J. Appl. Phys.* **100**, 114310 (2006).
- ⁴A. G. Milnes, *Deep Impurities in Semiconductors* (Wiley, New York, 1973).
- ⁵D. K. Schroder, *Semiconductor Material and Device Characterization* (Wiley, New York, 1990), p. 319.
- ⁶F. Scholtz, J. M. Hwang, and D. K. Schroder, *Solid-State Electron.* **31**, 205 (1988); F. J. Scholtz and J. W. Roach, *ibid.* **35**, 447 (1992).
- ⁷A. Van Der Ziel, *Fluctuation Phenomena in Semiconductors* (Academic, New York, 1959).
- ⁸P. Lauritzen and C. T. Shah, *IEEE Trans. Electron Devices* **10**, 334 (1963).
- ⁹J. A. Copland, *IEEE Trans. Electron Devices* **18**, 50 (1971).
- ¹⁰S. Reza, G. Bosman, M. S. Islam, T. I. Kamins, S. Sharma, and R. S. Williams, *IEEE Trans. Nanotechnol.* **5**, 1536 (2006).
- ¹¹H. D. Xiong, W. Wang, Q. Li, C. A. Richter, J. S. Suehle, W.-K. Hong, T. Lee, and D. M. Fleetwood, *Appl. Phys. Lett.* **91**, 053107 (2007).
- ¹²S. L. Rumyantsev, M. S. Shur, M. E. Levinshtein, A. Motayed, and A. V. Davydov, *J. Appl. Phys.* **103**, 064501 (2008).
- ¹³M. R. Sakr and X. P. A. Gao, *Appl. Phys. Lett.* **93**, 203503 (2008).
- ¹⁴D. Jang, H. W. Lee, K. Tachi, L. Montes, T. Ernst, G. T. Kim, and G. Ghibaudo, *Appl. Phys. Lett.* **93**, 073505 (2010).
- ¹⁵L. C. Li, K. H. Huang, Y. W. Suen, W. H. Hsieh, C. D. Chen, M. W. Lee, and C. C. Chen, *AIP Conf. Proc.* **893**, 731 (2007).
- ¹⁶A. Motayed, J. E. Bonevich, S. Krylyuk, A. V. Davydov, G. Aluri, and M. V. Rao, *Nanotechnology* **22**, 075206 (2011).
- ¹⁷Certain commercial equipments or material suppliers are identified in this paper for describing experimental procedure adequately. This does not imply endorsement by NIST.
- ¹⁸J. E. Allen, E. R. Hemesath, D. E. Perea, J. L. Lensch-Falk, Z. Y. Li, F. Yin, M. H. Gass, P. Wang, A. L. Bleloch, R. E. Palmer, and L. J. Lauhon, *Nat. Nanotechnol.* **3**, 168 (2008).
- ¹⁹E. C. Garnett, W. Liang, and P. Yang, *Adv. Mater.* **19**, 2946 (2007).
- ²⁰Y. Cui, X. Duan, J. Hu, and C. M. Lieber, *J. Phys. Chem. B* **104**, 5213 (2000).
- ²¹N. Lukyanchikova, *Source of the Lorentzian Components in the Low-frequency Noise Spectra of Submicron Metal-Oxide-Semiconductor Field-Effect Transistors, Noise and Fluctuations Control in Electronic Devices*, edited by A. Balandin (American Scientific, Riverside, CA, 2002).
- ²²G. Bemski, *Phys. Rev.* **111**, 1515 (1958).
- ²³M. Bullis, *Solid-State Electron.* **9**, 143 (1966).
- ²⁴A. Stolwijk, B. Schuster, and J. Hölzl, *Appl. Phys. A* **33**, 133 (1984).
- ²⁵C. Putnam, M. A. Filler, B. M. Kayes, M. D. Kelzenberg, Y. Guan, N. S. Lewis, J. M. Eiler, and H. A. Atwater, *Nano Lett.* **8**, 3109 (2008).
- ²⁶J. Pearton and A. J. Tavendale, *Phys. Rev. B* **26**, 7105 (1982).
- ²⁷See supplementary material at <http://dx.doi.org/10.1063/1.3637049> for the $\ln(R)$ vs. $1/k_B T$ plot and a discussion.